Inorg. Chem. **2004**, *43*, 2998–3004

Synthesis, Crystal Structures, and Optical Properties of Two New Layered Quaternary Tantalum Thiophosphates and the Thermal Conversion of $Cs_4Ta_4P_4S_{24}$ into $Cs_2Ta_2P_2S_{12}$

Andreas Gutzmann, Christian Näther, and Wolfgang Bensch*

Institut für Anorganische Chemie, Universität Kiel, Olshausenstr. 40, D-24098 Kiel, Germany

Received November 5, 2003

The reaction of Ta with an in situ formed polythiophosphate melt of Cs_2S_3, P_2S_5, and S yields the two new quaternary tantalum thiophosphates $Cs_2Ta_2P_2S_{12}$ (**I**) and $Cs_4Ta_4P_4S_{24}$ (**II**). Both compounds were obtained with the same stoichiometric ratio but at different reaction temperatures. Compound **I** was prepared at 873 K and crystallizes in the monoclinic space group $P2_1/c$ (No. 14) with $a = 8.862(2)$ Å, $b = 12.500(3)$ Å, $c = 17.408(4)$ Å, $\beta = 99.23(3)°$, and $Z = 4$. Compound **II** was prepared at 773 K and crystallizes in the monoclinic space group $P2_1/n$ (No. 14) with $a = 14.298(3)$ Å, $b = 17.730(4)$ Å, $c = 16.058(3)$ Å, $\beta = 106.19(3)°$, and $Z = 4$. The two structures are closely related and exhibit two-dimensional anionic layers consisting of dimeric $[Ta_2S_{11}]$ units which are linked by two tetradentate and two tridentate $[PS_4]$ tetrahedra. The significant difference between these two compounds is the orientation of the $[Ta_2S_{11}]$ units in infinite $[Ta_2S_4(PS_4)]_x$ chains which are subunits of both structures. The specific orientation of the $[Ta_2S_{11}]$ blocks in compound **I** leads to the formation of one cavity in the $^2_\infty[Ta_2P_2S_{12}]^{2-}$ layers, whereas in compound **II** two types of cavities are observed in the $^2_\infty[Ta_4P_4S_{24}]^{4-}$ layers. The Cs^+ ions are located between the layers above and below the cavities. The compounds were characterized with infrared spectroscopy in the MIR region, Raman spectroscopy, and UV/Vis diffuse reflectance spectroscopy. When $Cs_4Ta_4P_4S_{24}$ (**II**) is heated at the synthesis temperature of compound **I** it is fully converted into compound **I**.

Introduction

The use of the molten alkali metal polychalcophosphate flux method is a well-established synthetical tool to synthesize new quaternary chalcogenphoshates. The in-situ fusion of A_2Q_x, P_2Q_5, and Q (A = alkali metal, Q = S, Se) forms highly reactive, discrete $[P_yQ_z]^{n-}$ anions which in the presence of metal ions coordinate and become the building block of new structures. Group 5 metal thiophosphates are known for their low-dimensional crystal structures and interesting physical properties. In the structures of compounds in the A−M−P−S system (A = alkali metal, M = group 5 metal) the dimensionality of the anionic parts varies from one-dimensional chains to three-dimensional interconnected networks.[1−10] Very recently we reported the syntheses, structures, and properties of the new quaternary thiophosphates with group 5 metals, $Rb_2Nb_2P_2S_{11}$[1] and $Rb_4Ta_4P_4S_{24}$.[2] We demonstrated that a systematic variation of the reaction parameters, e.g., temperature, reaction time, and stoichiometry of the starting materials, leads to the formation of new quaternary thiophosphates with interesting structural features. Upon analyzing the structures of these compounds often $[M_2S_{11}]$ or $[M_2S_{12}]$ units and tetrahedral $[PS_4]^{3-}$ groups are found as the general structural motifs.[1,2,6−10] A highly interesting observation in the structures with group 5 metals is that in the overwhelming number of compounds only the $[PS_4]^{3-}$ anion occurs as the building unit. An exception is vanadium for which $[P_2S_6]^{4-}$ and $[P_2S_7]^{4-}$ anions were reported.[3−5] The well characterized $[P_yS_z]^{n-}$ species such as

* Author to whom correspondence should be addressed. Fax: +49-(0)-431-8801520. E-mail: wbensch@ac.uni-kiel.de.

(1) Gutzmann, A.; Bensch, W. *Solid State Sci.* **2002**, *4*, 835−840.
(2) Gutzmann, A.; Bensch, W. *Solid State Sci.* **2003**, *5*, 1271−1276.
(3) Kopnin, E.; Coste, S.; Jobic, S.; Evain, M.; Brec, R. *Mater. Res. Bull.* **2000**, *35*, 1401−1410.
(4) Durand, E.; Evain, M.; Brec, R. *J. Solid State Chem.* **1993**, *102*, 146−155.
(5) Tremel, W.; Kleinke, H.; Derstroff, V.; Reisner, C. *J. Alloys Compd.* **1995**, *219*, 73−82.
(6) Goh, E.-Y.; Kim, S.-J.; Jung, D. *J. Solid State Chem.* **2002**, *168*, 119−125.
(7) Do, J.; Yun, H. *Inorg. Chem.* **1996**, *35*, 3729−3730.
(8) Kim, C.; Yun, H. *Acta Crystallogr.* **2002**, *C58*, i53−i54.
(9) Derstroff, V.; Gieck, C.; Regelsky, G.; Ksenofontov, V.; Gütlich, P.; Eckert, H.; Tremel, W. *Chem. Eur. J.*, submitted for publication.
(10) Derstroff, V.; Tremel, W. *Chem. Commun.* **1998**, 913−914.

10.1021/ic035273k CCC: $27.50
Published on Web 03/17/2004

$[P_2S_6]^{2-}$, $[P_2S_8]^{4-}$, $[P_2S_9]^{4-}$, $[P_2S_{10}]^{4-}$, $[P_3S_9]^{3-}$, $[P_3S_{10}]^{5-}$, $[P_4S_{12}]^{4-}$, or $[P_4S_{13}]^{6-}$ [11−18] are never found in the quaternary group 5 thiophosphates. Therefore, we decided to investigate intensively the A−M−P−S family (A = alkali metal, M = group 5 metal). In our ongoing investigations of quaternary tantalum thiophosphates synthesized applying a polythiophosphate melt, we have obtained two new quaternary compounds: $Cs_2Ta_2P_2S_{12}$ (**I**) and $Cs_4Ta_4P_4S_{24}$ (**II**). Here we report the synthesis, the crystal structures, and the optical properties of these new quaternary thiophosphates.

Experimental Section

Synthesis. The following reagents were used as obtained: Cs (99.5%, Strem), Ta (99.97%, Fluka), P_2S_5 (99.99%, Alfa), S (99.99%, Heraeus). Cs_2S_3 was prepared from a stoichiometric ratio of the elements in liquid ammonia under an argon atmosphere. The compound $Cs_2Ta_2P_2S_{12}$ (**I**) was prepared by the reaction of 0.28 mmol Cs_2S_3, 0.56 mmol Ta, 0.28 mmol P_2S_5, and 1.1 mmol S. The reaction mixture was thoroughly mixed in a N_2-filled glovebox and loaded into a silica tube which was evacuated (1×10^{-3} mbar) and flame-sealed. The ampule was placed in a computer-controlled furnace and heated to 873 K within 18 h. After 4 days the sample was cooled to 523 K with 2 K h^{-1}, and then in 10 h to room temperature.

$Cs_4Ta_4P_4S_{24}$ (**II**) was prepared from a reaction of 0.25 mmol Cs_2S_3, 0.25 mmol Ta, 0.25 mmol P_2S_5, and 1.8 mmol S. The starting materials were loaded into a glass ampule (Duran) and were heated to 773 K for 6 days and then cooled to room temperature with a cooling rate of 3 K h^{-1}. To remove unreacted $Cs_xP_yS_z$ the resultant melt was washed with DMF and ether. The products (**I**) and (**II**) (yield: ∼70% based on Ta) consisted of orange crystals which are stable in air and moisture. A semiquantitative EDX analysis of single orange crystals indicated the presence of all four elements (Cs, Ta, P, and S) for both compounds in an approximate atomic ratio of 1:1:1:6.

Structure Determinations. Single-crystal X-ray diffraction data were collected using a STOE Image Plate Diffraction System (IPDS) (Mo Kα radiation; $\lambda = 0.71073$ Å). Structure solution was performed with SHELXS-97.[19] Refinement was done against F^2 using SHELXL-97.[19] All atoms were refined with anisotropic displacement parameters. Technical details of the data acquisition as well as some refinement results for compounds **I** and **II** are summarized in Table 1. Atomic coordinates and equivalent isotropic displacement parameters are given in Table 2 for compound **I** and in Table 3 for compound **II**.

Infrared Spectroscopy. Infrared spectra in the MIR region (4000−400 cm^{-1}, 2 cm^{-1} resolution) were collected on a Genesis FT-spectrometer (ATI Mattson). Single crystals of the compounds were ground together with KBr and pressed into a transparent pellet.

Solid-State UV/Vis/NIR Spectroscopy. UV/Vis-spectroscopic investigations were conducted at room temperature using a UV−Vis−NIR-two-channel spectrometer Cary 5 from Varian Techtron Pty., Darmstadt. The optical properties of the compounds were investigated by studying the UV/Vis reflectance spectrum of the powdered sample. The absorption data were calculated using the Kubelka−Munk relation for diffuse reflectance data. $BaSO_4$ powder was used as reference material.

Semiquantitative Microprobe Analyses. Semiquantitative microprobe analyses were performed using a Philips ESEM XL 30 scanning electron microscope equipped with an EDAX analyzer.

Table 1. Crystal Data and Structure Refinements for $Cs_2Ta_2P_2S_{12}$ (**I**) and $Cs_4Ta_4P_4S_{24}$ (**II**)

	$Cs_2Ta_2P_2S_{12}$	$Cs_4Ta_4P_4S_{24}$
fw	1074.38	2148.76
space group	$P2_1/c$	$P2_1/n$
a (Å)	8.862 (2)	14.298 (3)
b (Å)	12.500 (3)	17.730 (4)
c (Å)	17.408 (4)	16.058 (3)
β (deg)	99.23 (3)	106.19 (3)
V (Å^3)	1903.3 (7)	3909.2 (14)
Z	4	4
T (K)	293	293
D_{calc} (g/cm^3)	3.749	3.651
μ (mm^{-1})	16.72	16.28
R_{int}	0.0518	0.0582
R1 ($F_o > 4\sigma(F_o)$)	0.0540	0.0352
wR2 (all data)	0.1493	0.0891
GOF	1.024	1.014

Table 2. Atomic Coordinates and Equivalent Isotropic Displacement Parameters U_{eq} (Å^2·10^3)[a] for $Cs_2Ta_2P_2S_{12}$ (**I**)[b]

atom	x	y	z	U_{eq}
Ta(1)	0.1602(1)	0.1823(1)	0.1352(1)	21(1)
Ta(2)	−0.5913(1)	0.2408(1)	0.0079(1)	20(1)
Cs(1)	−0.3068(1)	0.3844(1)	0.2166(1)	39(1)
Cs(2)	0.1634(1)	0.5663(1)	0.1809(1)	63(1)
P(1)	−0.7049(3)	0.2627(2)	−0.1796(2)	24(1)
P(2)	−0.2208(3)	0.2557(2)	0.0051(2)	23(1)
S(1)	−0.7527(3)	0.3621(2)	−0.0944(2)	27(1)
S(2)	0.3965(3)	0.1546(2)	0.2394(2)	27(1)
S(3)	0.1063(3)	0.2962(2)	0.2493(2)	27(1)
S(4)	0.0156(3)	0.0462(2)	0.1554(2)	32(1)
S(5)	−0.0427(3)	0.3222(2)	0.0821(2)	27(1)
S(6)	−0.5710(3)	0.1455(2)	−0.1246(2)	30(1)
S(7)	0.1567(3)	0.1347(2)	−0.0054(2)	24(1)
S(8)	−0.6597(3)	0.0705(2)	0.0687(2)	24(1)
S(9)	−0.3467(3)	0.1522(2)	0.0640(2)	27(1)
S(10)	−0.3857(3)	0.3723(2)	−0.0210(2)	28(1)
S(11)	−0.1494(3)	0.1902(2)	−0.0853(2)	33(1)
S(12)	−0.6629(3)	0.3491(2)	0.0993(2)	24(1)

[a] The U_{eq} is defined as one-third of the trace of the orthogonalized U_{ij} tensor. [b] Estimated standards deviations are given in parentheses.

Results and Discussion

Crystal Structures. $Cs_2Ta_2P_2S_{12}$ (**I**) crystallizes in the monoclinic space group $P2_1/c$ with 4 formula units in the cell. The two crystallographically independent Cs, Ta, and P atoms as well as the 12 unique S atoms of compound (**I**) are located on general positions. In the structure $^2_\infty[Ta_2P_2S_{12}]^{2-}$ anionic layers are found which are separated by the Cs cations (Figure 1).

The layers are formed by the interconnection of dimeric $[Ta_2S_{11}]$ units and $[PS_4]$ tetrahedra. Each Ta atom is

(11) Brockner, W.; Becker, R.; Eisenmann, B.; Schaefer, H. *Z. Anorg. Allg. Chem.* **1985**, *520*, 51−58.
(12) Brec, R.; Grenouilleau, P.; Evain, M.; Rouxel, J. *Rev. Chim. Min.* **1983**, *20*, 295−304.
(13) Derstroff, V.; Tremel, W.; Regelsky, G.; Schmedt auf der Günne, J.; Eckert, H. *Solid State Sci.* **2002**, *4*, 731−745.
(14) Aitken, J. A.; Canlas, C.; Weliky, D. P.; Kanatzidis, M. G. *Inorg. Chem.* **2001**, *40*, 6496−6498.
(15) Hanko, J. A.; Sayettat, J.; Jobic, S.; Brec, R.; Kanatzidis, M. G. *Chem. Mater.* **1998**, *10*, 3040−3049.
(16) Hess, R. F.; Abney, K. D.; Burris, J. L.; Hochheimer, H. D.; Dorhout, P. K. *Inorg. Chem.* **2001**, *40*, 2851−2859.
(17) Evain, M.; Brec, R.; Ouvrard, G.; Rouxel, J. *Mater. Res. Bull.* **1984**, *19*, 41−48.
(18) Evain, M.; Brec, R.; Ouvrard, G.; Rouxel, J. *J. Solid State Chem.* **1985**, *56*, 12−20.
(19) Sheldrick, G. M. *SHELXL97 and SHELXS97*; University of Göttingen, Germany, 1997.

Table 3. Atomic Coordinates and Equivalent Isotropic Displacement Parameters U_{eq} ($Å^2 \cdot 10^3$)[a] for $Cs_4Ta_4P_4S_{24}$ (**II**)[b]

atom	x	y	z	U_{eq}
Ta(1)	0.2500(1)	0.3909(1)	0.7575(1)	13(1)
Ta(2)	0.1345(1)	0.2279(1)	0.8094(1)	12(1)
Ta(3)	0.1714(1)	0.3763(1)	1.3409(1)	13(1)
Ta(4)	0.2120(1)	0.2130(1)	1.2340(1)	14(1)
Cs(1)	0.4934(1)	0.5163(1)	0.6239(1)	28(1)
Cs(2)	−0.1318(1)	0.3336(1)	1.0322(1)	36(1)
Cs(3)	0.3589(1)	0.4374(1)	1.0489(1)	38(1)
Cs(4)	−0.0564(1)	0.3720(1)	0.5018(1)	49(1)
P(1)	0.2953(2)	0.0423(2)	1.2983(2)	21(1)
P(2)	0.3099(2)	0.5652(1)	0.8314(2)	15(1)
P(3)	0.1578(2)	0.2166(2)	1.0190(2)	16(1)
P(4)	0.2523(2)	0.3893(1)	1.5526(2)	14(1)
S(1)	0.1374(2)	0.2898(1)	0.6708(2)	18(1)
S(2)	0.2003(2)	0.1425(1)	0.9380(2)	17(1)
S(3)	0.1801(2)	0.1049(2)	1.3215(2)	23(1)
S(4)	0.2758(2)	0.4479(2)	1.2618(2)	20(1)
S(5)	0.3193(2)	0.2816(1)	1.3339(2)	18(1)
S(6)	0.1016(2)	0.3286(2)	1.1909(2)	20(1)
S(7)	0.3906(2)	0.4824(1)	0.7922(2)	21(1)
S(8)	0.0016(2)	0.1680(2)	0.7428(2)	20(1)
S(9)	0.0659(2)	0.2603(1)	1.2808(2)	19(1)
S(10)	0.2564(2)	0.1400(1)	0.7658(2)	20(1)
S(11)	0.3031(2)	0.4415(2)	1.4604(2)	23(1)
S(12)	0.0753(2)	0.3570(1)	0.7454(2)	18(1)
S(13)	0.0864(2)	0.2952(2)	0.9314(2)	24(1)
S(14)	0.1921(2)	0.4963(1)	0.8335(2)	19(1)
S(15)	0.1769(2)	0.4611(1)	0.6090(2)	17(1)
S(16)	0.1705(2)	0.3053(1)	1.4771(2)	17(1)
S(17)	0.3545(2)	0.3449(2)	0.6569(2)	18(1)
S(18)	0.0760(2)	0.1678(2)	1.0891(2)	24(1)
S(19)	0.3113(2)	0.3046(2)	0.8616(2)	20(1)
S(20)	0.2755(2)	0.2620(2)	1.1087(2)	22(1)
S(21)	0.3252(3)	0.1160(2)	1.2095(2)	30(1)
S(22)	0.0531(2)	0.4558(2)	1.3348(2)	27(1)
S(23)	0.3772(2)	0.6137(2)	0.9427(2)	26(1)
S(24)	0.4011(4)	0.0173(3)	1.4010(3)	60(1)

[a] The U_{eq} is defined as one-third of the trace of the orthogonalized U_{ij} tensor. [b] Estimated standards deviations are given in parentheses.

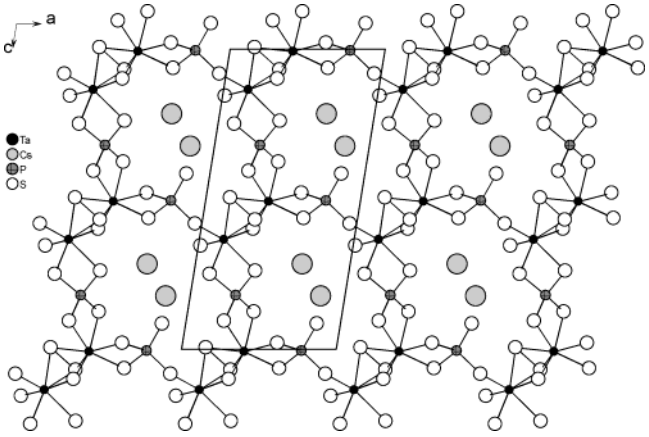

Figure 1. Crystal structure of $Cs_2Ta_2P_2S_{12}$ (**I**) with view along [0 1 0].

surrounded by one μ_2-η^2, η^2-S_2^{2-} anion, one μ_2-S^{2-} ion, and four terminal S^{2-} anions in a distorted pentagonal bipyramidal environment (Figures 2 and 3, left). Two of these distorted [TaS_7] groups share a triangular face made of mono- and disulfide anions to form the dimeric [Ta_2S_{11}] units. Hence, the coordination mode can be described as [$Ta_2(\mu_2$-$S)(\mu_2$-η^2,η^2-$S_2)(S)_8]^{4-}$.

The Ta(1) atom is 0.315 Å below the pentagonal plane formed by S2−S3−S5−S7−S8, whereas the Ta(2) atom is

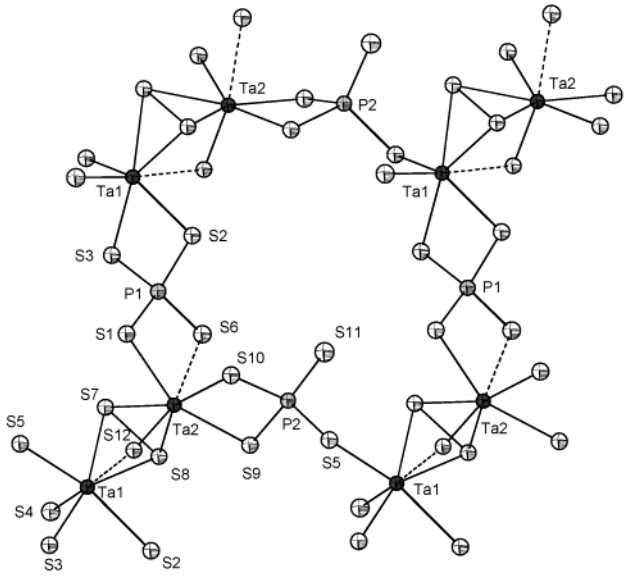

Figure 2. Interconnection of the [Ta_2S_{11}] units by [PS_4] tetrahedra in Cs_2-$Ta_2P_2S_{12}$ (**I**) with atomic labeling. The ellipsoids are drawn at the 50% probability level. The dashed lines represent the longest Ta−S bonds.

0.219 Å above the pentagonal plane formed by S1−S7−S8−S9−S10. The angle between these two planes is 72.3°. The Ta−S bond lengths range from 2.192(3) to 2.740(3) Å. Each of the two unique Ta atoms has a short bond to a sulfur atom (S(4) and S(12)) of about 2.2 Å. We note that the short bond of Ta(1) is to the terminal $S(4)^{2-}$ anion, whereas Ta(2) has the shortest bond to the μ-$S(12)^{2-}$ anion which is bound to Ta(1) (Table 4, Figure 2). These short distances match well with those reported for compounds containing the complex anion $[Ta_2S_{11}]^{4-}$. [20−22]

The longest Ta−S bonds of 2.740(3) Å for Ta(1)−S(12) and 2.629(3) Å for Ta(2)−S(6) are observed in trans position to the short Ta−S bonds. Again, this Ta−S bond lengths pattern was also found in compounds with the $[Ta_2S_{11}]^{4-}$ anion.[20−22] We note that the coordination mode of the metal centers in the pentagonal bipyramid of the ternary sulfides $A_4M_2S_{11}$ (A = K, Rb, Cs, Tl; M = Nb, Ta) is quite different.[20−24] In both pentagonal planes of the $[M_2S_{11}]^{4-}$ anion are one η^2-S_2^{2-} unit, one μ_2-S^{2-} anion bridging the two M^{5+} atoms, and one (μ_2-η^2,η^1-S_2) anion which is η^2 to one M^{5+} while one S atom of this unit serves as a bridging atom to the second M center (Figure 3, right). Therefore, the connection mode for these $[Ta_2S_{11}]^{4-}$ anions may be described as $[Ta_2(\mu_2$-$S)(\mu_2$-η^2,η^1-$S_2)_2(\eta^2$-$S_2)_2(S)_2]^{4-}$. In the pentagonal planes of compound **I** are three S^{2-} anions and one (μ_2-η^2,η^2-S_2) anion which is η^2 to both Ta atoms. The μ_2-S^{2-} unit bridging the two Ta atoms is moved out of the pentagonal plane and is located in axial position (Figure 3, left). From a formal point of view the S_2^{2-} anions in the

(20) Herzog, S.; Näther, C.; Bensch, W. *Z. Anorg. Allg. Chem.* **1999**, *625*, 969−974.
(21) Dürichen, P.; Bensch, W. *Acta Crystallogr.* **1998**, *C54*, 706−708.
(22) Teske, C. L.; Bensch, W. *Z. Anorg. Allg. Chem.* **2001**, *627*, 385−389.
(23) Bensch, W.; Dürichen, P. *Eur. J. Solid State Inorg. Chem.* **1996**, *33*, 527−536.
(24) Bensch, W.; Dürichen, P.; Näther, C. *Solid State Sci.* **1999**, *1*, 85−108.

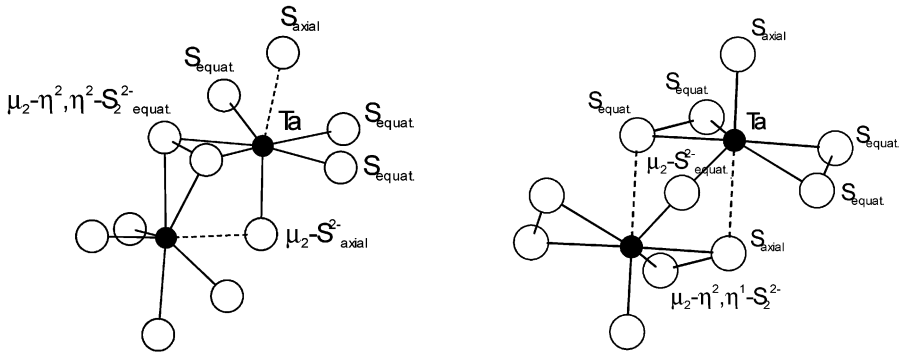

Figure 3. Crystal structure of the $[Ta_2S_{11}]^{4-}$ anion in $Cs_2Ta_2P_2S_{12}$ (**I**) (left) and $A_4Ta_2S_{11}$ (A = alkali metal, Tl) (right). The dashed lines represent the longest Ta−S bonds.

Table 4. Selected Distances (Å) and Angles (deg) for $Cs_2Ta_2P_2S_{12}$ (**I**)

Ta(1)−S(2)	2.564(3)	Ta(1)−S(3)	2.551(3)
Ta(1)−S(4)	2.192(3)	Ta(1)−S(5)	2.572(3)
Ta(1)−S(7)	2.514(3)	Ta(1)−S(8)	2.536(3)
Ta(1)−S(12)	2.740(3)	Ta(2)−S(1)	2.588(3)
Ta(2)−S(6)	2.629(3)	Ta(2)−S(7)	2.576(3)
Ta(2)−S(8)	2.495(3)	Ta(2)−S(9)	2.490(3)
Ta(2)−S(10)	2.563(3)	Ta(2)−S(12)	2.255(3)
S(7)−S(8)	2.069(4)		
P(1)−S(1)	2.031(4)	P(1)−S(2)	2.067(4)
P(1)−S(3)	2.052(4)	P(1)−S(6)	2.026(4)
P(2)−S(5)	2.073(4)	P(2)−S(9)	2.082(4)
P(2)−S(10)	2.062(4)	P(2)−S(11)	1.967(4)
S(1)−P(1)−S(2)	110.9(2)	S(1)−P(1)−S(3)	114.5(2)
S(3)−P(1)−S(2)	99.8(2)	S(6)−P(1)−S(1)	105.8(2)
S(6)−P(1)−S(2)	113.5(2)	S(6)−P(1)−S(3)	112.6(2)
S(5)−P(2)−S(9)	110.1(2)	S(10)−P(2)−S(5)	107.3(2)
S(10)−P(2)−S(9)	97.5(2)	S(11)−P(2)−S(5)	112.0(2)
S(11)−P(2)−S(9)	113.7(2)	S(11)−P(2)−S(10)	115.2(2)

$[M_2S_{11}]^{4-}$ groups are oxidized followed by a pronounced rearrangement of the ligands within the $[M_2S_{11}]$ unit.

The S−S bond length in the S_2^{2-} anion amounts to 2.069(4) Å and is in the expected range for a S−S single bond (Table 4). The Ta−Ta distance within the $[Ta_2S_{11}]$ units amounts to 3.443(2) Å, which is too long for metal-to-metal interactions [$r(Ta^{5+}) = 0.69$ Å].[25]

The most interesting feature of the structure is the connection scheme of the $[Ta_2S_{11}]$ units via $[PS_4]$ tetrahedra. Each $[Ta_2S_{11}]$ group shares common edges with two tetradentate $[PS_4]$ tetrahedra, a common corner as well as a common edge with two tridentate $[PS_4]$ tetrahedra. The interconnection of the $[Ta_2S_{11}]$ units via the tridentate $P(2)S_4^{3-}$ anions yields infinite $[Ta_2S_4(P(2)S_4)]_x$ chains running parallel to the crystallographic *a* axis (Figure 4). On the other hand, the connection of the $[Ta_2S_{11}]$ building blocks via the tetradentate $P(1)S_4^{3-}$ anions leads to the formation of another chain $[Ta_2S_4(P(1)S_4)]_x$ which is directed along the *c* axis. In neighboring chains the $[Ta_2S_{11}]$ building blocks exhibit the same orientation (Figure 4). In addition, the terminal S atom of the $P(2)S_4^{3-}$ anion in the $[Ta_2S_4(P(2)S_4)]_x$ chain always points into the same direction (Figure 4).

The layered $^2_\infty[Ta_2P_2S_{12}]^{2-}$ anion extending within the (010) plane may be viewed as the condensation product of two chains that are running parallel to different crystallographic directions. The distinct connection scheme leads to the formation of cavities within the layers with approximate diameters of about 6.75−9.17 Å (measured from coordinate to coordinate) (Figure 4).

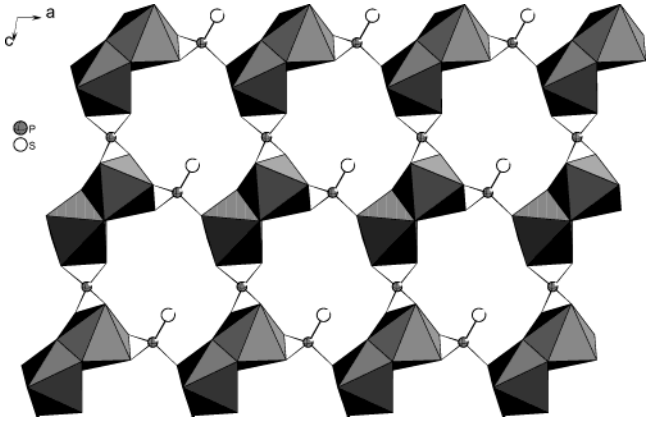

Figure 4. Interconnection of the $[Ta_2S_{11}]$ units via tridentate $[PS_4]$ tetrahedra in $Cs_2Ta_2P_2S_{12}$ (**I**) parallel to the crystallographic *a* axis and the interconnection of the individual chains by the tetradentate $[PS_4]$ tetrahedra. Cs^+ cations are omitted for clarity.

The average P−S bond lengths in the two unique PS_4^{3-} anions amount to 2.044 and 2.046 Å (Table 4). The individual P−S distances range from 1.967(4) (P−S_t, t = terminal) to 2.082(4) Å (P−S_{br}, br = bridging) (Table 4). The $[PS_4]$ tetrahedra are strongly distorted as is evidenced by the S−P−S angles between 97.5(2) and 115.2(2)° (Table 4). These distortions of the tetrahedra are similar to those found in other $[PS_4]$ containing compounds.[8,26,27]

The two crystallographically independent alkali metal cations are in an 11-fold coordination (Cs(1), average Cs(1)−S distance 3.785 Å), and a 9-fold coordination (Cs(2), average Cs(2)−S distance 3.735 Å). The Cs^+ cations are located above and below the cavities. The average Cs−S bond lengths are in agreement with the sum of the ionic radii.[25]

The structure of $Cs_4Ta_4P_4S_{24}$ (**II**) (Figure 5) is isotypic to that of $Rb_4Ta_4P_4S_{24}$.[2] In the structure $^2_\infty[Ta_4P_4S_{24}]^{4-}$ anionic layers are separated by Cs atoms. The layers are also built of dimeric $[Ta_2S_{11}]$ units and $[PS_4]$ tetrahedra. The Ta−S distances of the two distinct $[Ta_2S_{11}]$ building blocks range from 2.179(3) to 2.786(3) Å. Each of the four crystallo-

(25) Shannon, R. D. *Acta Crystallogr.* **1976**, *A32*, 751−767.

(26) Cieren, X.; Angenault, J.; Couturier, J.-C.; Jaulmes, S.; Quarton, M.; Robert, F. *J. Solid State Chem.* **1996**, *121*, 230−235.

(27) Derstroff, V.; Ensling, J.; Ksenofontov, V.; Gütlich, P.; Tremel, W. *Z. Anorg. Allg. Chem.* **2002**, *628*, 1346−1354.

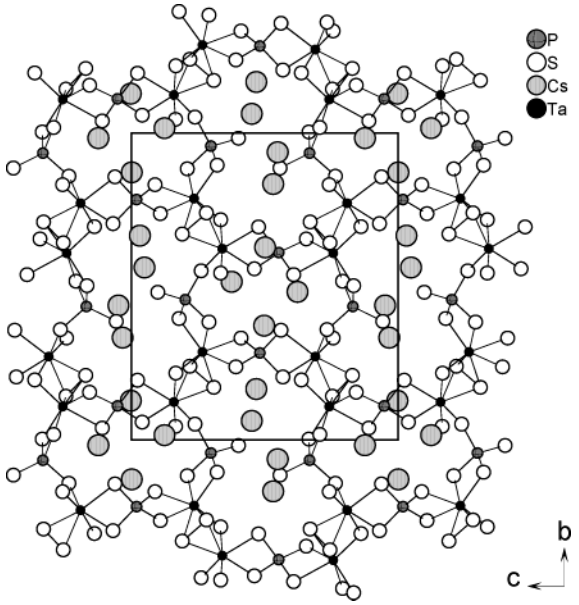

Figure 5. Crystal structure of $Cs_4Ta_4P_4S_{24}$ (**II**) with view along [1 0 0].

Table 5. Selected Distances (Å) and Angles (deg) for $Cs_4Ta_4P_4S_{24}$ (**II**)

Ta(1)−S(1)	2.548(3)	Ta(1)−S(7)	2.521(3)
Ta(1)−S(12)	2.524(3)	Ta(1)−S(14)	2.498(3)
Ta(1)−S(15)	2.633(2)	Ta(1)−S(17)	2.617(3)
Ta(1)−S(19)	2.254(3)	Ta(2)−S(1)	2.492(2)
Ta(2)−S(2)	2.522(2)	Ta(2)−S(8)	2.179(3)
Ta(2)−S(10)	2.577(3)	Ta(2)−S(12)	2.555(3)
Ta(2)−S(13)	2.546(3)	Ta(2)−S(19)	2.786(3)
Ta(3)−S(4)	2.551(3)	Ta(3)−S(5)	2.727(3)
Ta(3)−S(6)	2.484(3)	Ta(3)−S(9)	2.574(3)
Ta(3)−S(11)	2.559(3)	Ta(3)−S(16)	2.527(2)
Ta(3)−S(22)	2.183(3)	Ta(4)−S(3)	2.491(3)
Ta(4)−S(5)	2.244(3)	Ta(4)−S(6)	2.562(3)
Ta(4)−S(9)	2.550(3)	Ta(4)−S(18)	2.704(3)
Ta(4)−S(20)	2.579(3)	Ta(4)−S(21)	2.468(3)
S(1)−S(12)	2.059(4)	S(6)−S(9)	2.056(4)
P(1)−S(3)	2.104(4)	P(1)−S(4)	2.055(4)
P(1)−S(21)	2.064(4)	P(1)−S(24)	1.953(5)
P(2)−S(7)	2.071(4)	P(2)−S(10)	2.066(4)
P(2)−S(14)	2.089(4)	P(2)−S(23)	1.975(4)
P(3)−S(2)	2.058(4)	P(3)−S(13)	2.041(4)
P(3)−S(18)	2.029(4)	P(3)−S(20)	2.050(4)
P(4)−S(11)	2.043(4)	P(4)−S(15)	2.037(4)
P(4)−S(16)	2.066(4)	P(4)−S(17)	2.048(4)
S(4)−P(1)−S(3)	101.7(2)	S(4)−P(1)−S(21)	111.2(2)
S(21)−P(1)−S(3)	96.4(2)	S(24)−P(1)−S(3)	115.5(2)
S(24)−P(1)−S(4)	112.1(2)	S(24)−P(1)−S(21)	117.8(3)
S(7)−P(2)−S(14)	96.4(2)	S(10)−P(2)−S(7)	113.7(2)
S(10)−P(2)−S(14)	100.7(2)	S(23)−P(2)−S(7)	114.3(2)
S(23)−P(2)−S(10)	114.2(2)	S(23)−P(2)−S(14)	115.6(2)
S(13)−P(3)−S(2)	100.3(2)	S(13)−P(3)−S(20)	111.8(2)
S(18)−P(3)−S(2)	113.4(2)	S(18)−P(3)−S(13)	114.8(2)
S(18)−P(3)−S(20)	105.4(2)	S(20)−P(3)−S(2)	111.4(2)
S(11)−P(4)−S(16)	99.1(2)	S(11)−P(4)−S(17)	116.8(2)
S(15)−P(4)−S(11)	112.2(2)	S(15)−P(4)−S(16)	115.4(2)
S(15)−P(4)−S(17)	102.8(2)	S(17)−P(4)−S(16)	111.2(2)

graphically independent Ta atoms has a short bond to a sulfur atom (S(19), S(8), S(22), and S(5)) and the longest Ta−S bonds are again situated in trans position to the short Ta−S bonds (Table 5, Figure 6).

The Ta−Ta separations within the $[Ta_2S_{11}]$ units amount to 3.5407(7) Å for Ta(1)−Ta(2) and 3.4956(7) Å for Ta(3)−Ta(4) and they are a little bit longer than those in compound **I**. The S−S bond lengths in the S_2^{2-} anions of 2.059(4) and 2.056(4) Å are typical for a S−S single bond

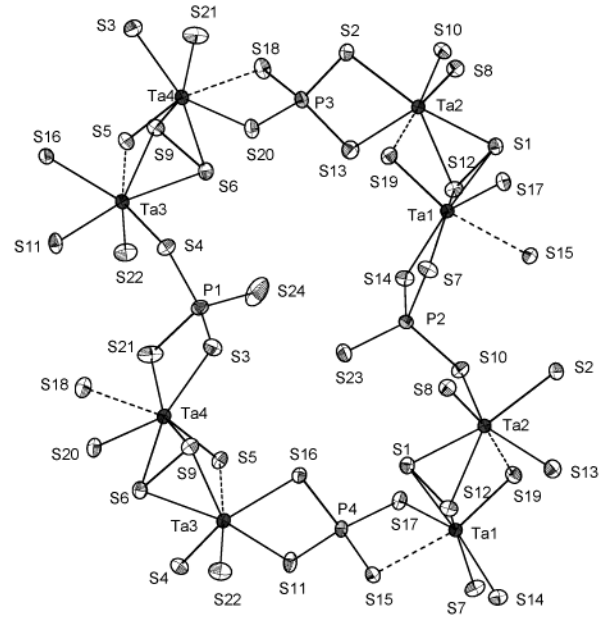

Figure 6. Interconnection of the two distinct $[Ta_2S_{11}]$ units by $[PS_4]$ tetrahedra in $Cs_4Ta_4P_4S_{24}$ (**II**) with atomic labeling. The ellipsoids are drawn at the 50% probability level. The dashed lines represent the longest Ta−S bonds.

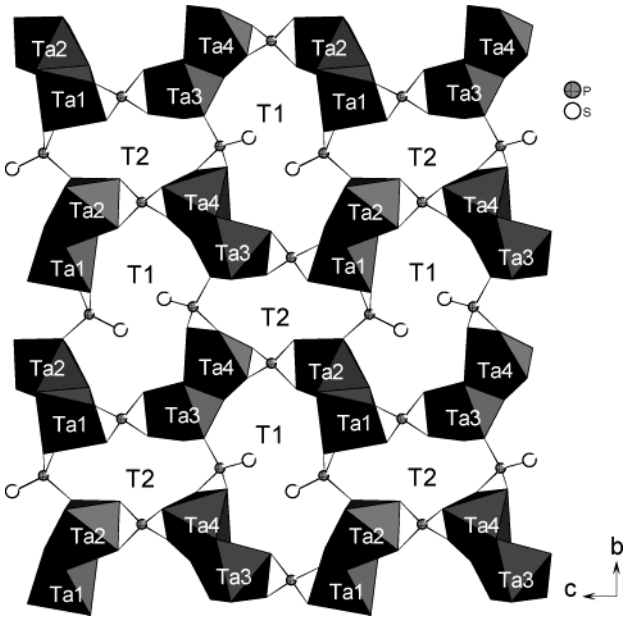

Figure 7. Interconnection of the $[Ta_2S_{11}]$ units via tridentate $[PS_4]$ tetrahedra in $Cs_4Ta_4P_4S_{24}$ (**II**) parallel to the crystallographic *b* axis and the interconnection of the individual chains by the tetradentate $[PS_4]$ tetrahedra. Cs^+ cations are omitted for clarity.

(Table 5). The binding mode in the $[Ta_2S_{11}]$ groups may be described as $[Ta_2(\mu_2\text{-}S)(\mu_2\text{-}\eta^2,\eta^2\text{-}S_2)(S)_8]^{4-}$ and is identical with that found in **I**.

The connection mode between the $[Ta_2S_{11}]$ and $[PS_4]$ groups in compound **II** is closely related to that in compound **I**. Again, two infinite $[Ta_2S_4(PS_4)]_x$ chains are observed which are condensed to form the layered anion. One chain contains only $[Ta(1,2)S_{11}]$ or $[Ta(3,4)S_{11}]$ units and is directed along the *b* axis. In the second chain along the *c* axis $[Ta(1,2)S_{11}]$ and $[Ta(3,4)S_{11}]$ groups alternate (Figure 7). The P−S bond lengths range from 1.953(5) (P−S_t, t = terminal, average

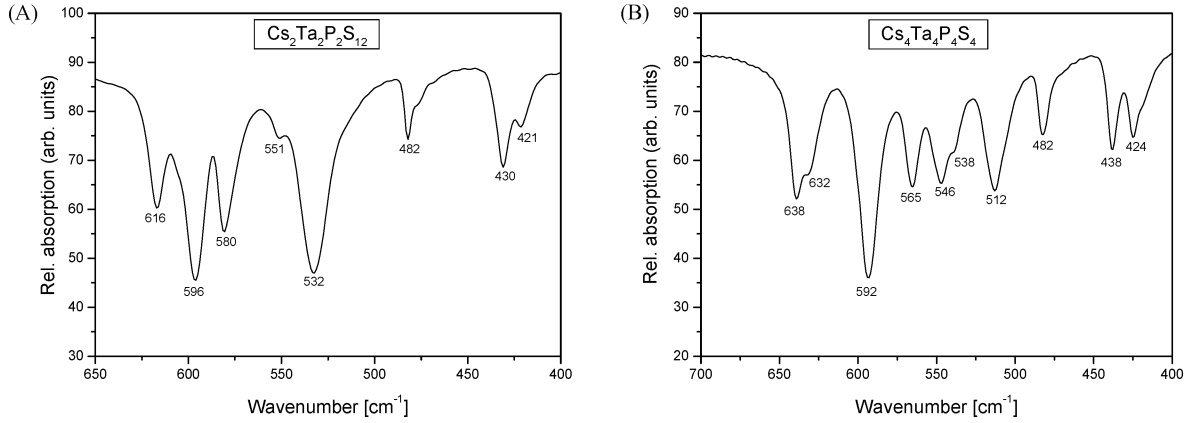

Figure 8. MIR spectra of $Cs_2Ta_2P_2S_{12}$ (**I**) (A) and $Cs_4Ta_4P_4S_{24}$ (**II**) (B).

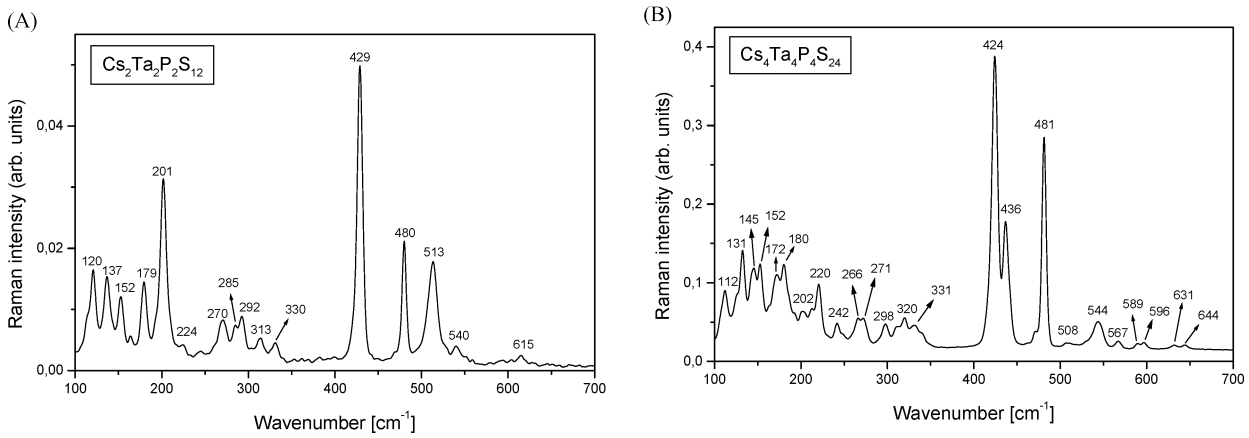

Figure 9. Raman spectra of $Cs_2Ta_2P_2S_{12}$ (**I**) (A) and $Cs_4Ta_4P_4S_{24}$ (**II**) (B).

P−S_t 1.964 Å) to 2.104(4) Å (P−S_{br}, br = bridging, average P−S_{br} 2.059 Å) (Table 5) and are comparable with those observed in **I** and other thiophosphates.[1,2,8,10] However, there are significant differences between the structures of **I** and **II**. In **II** the $[Ta_2S_{11}]$ units change their orientation within the individual chains (compare Figures 4 and 7). The terminal S atom of the $P(2)S_4^{3-}$ anion joining the $[Ta(1,2)S_{11}]$ units along the *b* axis shows a left-right-left orientation (Figure 7) whereas the $P(1)S_4^{3-}$ anion interconnecting the $[Ta(3,4)S_{11}]$ blocks exhibits a right-left-right orientation (Figure 7).

A consequence of the distinct arrangement of the chains is the formation of layers with two types of cavities (T1, T2) (Figure 7). The larger cavity (T1) with an ellipsoidal shape has a diameter of about 4.09−9.65 Å (measured from coordinate to coordinate) and the smaller is nearly rectangular (T2) with dimensions of about 3.84−8.13 Å.

The four crystallographically independent Cs cations are located between the layers above and below the cavities. With a cutoff of 4.2 Å the Cs^+ ions are in a 9-fold coordination (Cs(1), average Cs(1)−S distance 3.586 Å; Cs(3), average Cs(3)−S distance 3.769 Å), in a 10-fold coordination (Cs(2), average Cs(2)−S distance 3.781 Å) and in a 12-fold coordination (Cs(4), average Cs(4)−S distance 3.807 Å).

The density of compound **II** is significantly lower than that of **I** (Table 1). It can be assumed that the special arrangement of the bulky $[Ta_2S_{11}]$ units in **II** and the occurrence of two different cavities are responsible for the less dense packing of the constituents.

A comparison with the geometrical parameters of the isostructural compound $Rb_4Ta_4P_4S_{24}$ reveals only a slight influence of the Rb^+ ions onto the geometric parameters of the layered anion. Because of the smaller ionic radius of Rb^+ the unit cell parameters are slightly shorter and the unit cell volume is lower. The Ta−S bond lengths in $Rb_4Ta_4P_4S_{24}$ range from 2.172(2) to 2.770(2) Å (average 2.508 Å) and agree well with those found in compound **II**.

Optical Properties. The MIR spectra of $Cs_2Ta_2P_2S_{12}$ (**I**) and $Cs_4Ta_4P_4S_{24}$ (**II**) are shown in Figure 8. The spectrum of **I** displays absorptions at ca. 616, 596, 580, 551, 532, 482, 430, and 421 cm^{-1}. Using the data published for other $[PS_4]$ containing compounds, the signals at 421, 430, 482, 532, 551, 596, and 616 cm^{-1} may be assigned to P−S stretching vibrations.[16,27−31] The remaining signal at 580 cm^{-1} is attributed to a S−S stretching mode.[32]

The spectrum of compound **II** exhibits absorptions at 638, 632, 592, 565, 546, 538, 512, 482, 438, and 424 cm^{-1}. The most intense absorption at 592 and the weak peak at 538

(28) McCarthy, T.; Kanatzidis, M. G. *J. Alloys Compd.* **1996**, *236*, 70−85.
(29) Löken, S.; Tremel, W. *Eur. J. Inorg. Chem.* **1998**, 283−289.
(30) Gieck, C.; Tremel, W. *Chem. Eur. J.* **2002**, *8* (13), 2980−2987.
(31) Evain, M.; Queignec, M.; Brec, R. *J. Solid State Chem.* **1988**, *75*, 413−431.

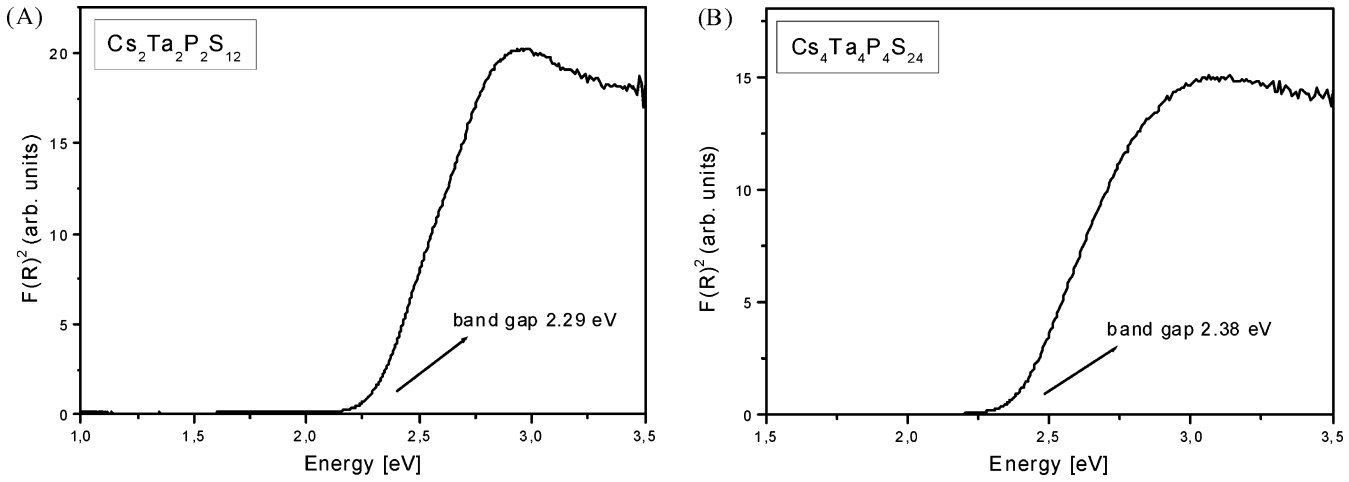

Figure 10. Transformed reflectance spectra of (A) $Cs_2Ta_2P_2S_{12}$ (**I**) and (B) $Cs_4Ta_4P_4S_{24}$ (**II**).

cm^{-1} are due to S−S stretching vibrations.[32] The remaining signals may be assigned to P−S stretching modes. The MIR spectrum of **II** is in good agreement with that of $Rb_4Ta_4P_4S_{24}$.[2]

Raman spectra of $Cs_2Ta_2P_2S_{12}$ (**I**) and $Cs_4Ta_4P_4S_{24}$ (**II**) are shown in Figure 9. In the spectrum of **I** very strong absorptions are located at 201, 429, 480, and 513 cm^{-1}. Resonances at lower energies (330−120 cm^{-1}) may be assigned to the S−P−S deformation modes of the $[PS_4]$ tetrahedra and the Ta−S stretching vibrations. The additional peak at 513 cm^{-1} can be tentatively assigned to a P−S stretching mode. Compound **II** exhibits strong absorptions at 424, 436, and 481 cm^{-1} which can be assigned to P−S stretching vibrations. The spectrum of **II** is in good agreement with the observed MIR data and the Raman spectrum of $Rb_4Ta_4P_4S_{24}$.[2]

The UV/vis diffuse reflectance spectra of **I** and **II** are shown in Figure 10. The band gaps were estimated to approximately 2.29 eV (541 nm) for **I** and 2.38 eV (521 nm) for **II**. These values are in good agreement with the orange color of the crystals.

Thermal Properties. Further investigations have shown that $Cs_4Ta_4P_4S_{24}$ (**II**) is also obtained with the same stoichiometric ratio as $Cs_2Ta_2P_2S_{12}$ (**I**) at 773 K. This indicates that the formation of the structure depends on the temperature. Therefore, we investigated the possibility of a thermal conversion of compound **II** into compound **I**. In previous investigations with respect to the thermal behavior of ternary group 5 chalcogenides we have demonstrated that the directed thermal decomposition of compounds is a synthetical tool for the preparation of new compounds.[33] Compound **II** was loaded into a silica tube which was evacuated to10^{-3} mbar and flame-sealed. The sample was heated to 873 K within 18 h and held at this temperature for 2 days. After cooling to room temperature (cooling rate 3 K h^{-1}) the product was investigated with X-ray powder diffractometry. The diffraction pattern of the material could be fully indexed on the basis of the pattern of compound **I**. According to the result of this experiment and as expected from the differing densities the thermodynamically more stable compound at room temperature should be **I**.

Summary

Two new quaternary tantalum thiophosphates $Cs_2Ta_2P_2S_{12}$ (**I**) and $Cs_4Ta_4P_4S_{24}$ (**II**) were prepared by applying an in situ formed melt containing $[P_xS_y]$ units, demonstrating the large potential of the synthesis method for the preparation of new and interesting compounds. An interesting observation is that in the structures only $[PS_4]^{3-}$ anions are found which act as tridentate or tetradentate ligands. The $[Ta_2S_{11}]$ units in the two compounds are interconnected by the $[PS_4]$ units in a different fashion and in the layered anions different cavities are formed. In compound **I** only one type of pore is observed, whereas the specific arrangement of the different building units in **II** leads to the formation of two different cavities. Interestingly, when $Cs_4Ta_4P_4S_{24}$ (**II**) is heated to 873 K it is fully converted into **I**. Further syntheses are under way to explore the quaternary group 5 thiophosphate system with the aim to prepare compounds that contain other $[P_xS_y]$ groups.

Acknowledgment. This research was supported by the State of Schleswig-Holstein and the Deutsche Forschungsgemeinschaft (DFG). We also thank I. Jeβ for the measurement of the single crystal data.

Supporting Information Available: Tables of atomic coordinates, isotropic and anisotropic displacement parameters, and full bond lengths and angles (including details of the structure determinations) for compounds **I** and **II** (pdf) and crystallographic files for both (cif). This material is available free of charge via the Internet at http://pubs.acs.org.

IC035273K

(32) Müller, A.; Jaegermann, W.; Enemark, J. H. *Coord. Chem. Rev.* **1982**, *46*, 245−280.
(33) Stoll, P.; Näther, C.; Jess, I.; Bensch, W. *Solid State Sci.* **2000**, *2*, 563−568.